Materials Horizons

Strain-triggered acidification in a double-network hydrogel enabled by multi-functional transduction of molecular mechanochemistry

Journal:	*Materials Horizons*
Manuscript ID	MH-COM-09-2022-001105.R1
Article Type:	Communication
Date Submitted by the Author:	22-Nov-2022
Complete List of Authors:	Ouchi, Tetsu; Duke University, Chemistry Bowser, Brandon; Duke University, Department of Chemistry Kouznetsova, Tatiana; Duke University, Chemistry Zheng, Xujun; Duke University Craig, Stephen; Duke University, Department of Chemistry

COMMUNICATION

Strain-triggered acidification in a double-network hydrogel enabled by multi-functional transduction of molecular mechanochemistry†

Received 00th January 20xx,
Accepted 00th January 20xx

DOI: 10.1039/x0xx00000x

Tetsu Ouchi,‡ Brandon H. Bowser,‡ Tatiana B. Kouznetsova, Xujun Zheng and Stephen L. Craig*

Recent work has demonstrated that force-triggered mechanochemical reactions within a polymeric material are capable of inducing measurable changes in macroscopic material properties, but examples of bulk property changes without irreversible changes in shape or structure are rare. Here, we report a double-network hydrogel that undergoes order-of-magnitude increases in acidity when strained, while recovering its initial shape after large deformation. The enabling mechanophore design is a 2-methoxy-gem-dichlorocyclopropane mechanoacid that is gated within a fused methyl methoxycyclobutene carboxylate mechanophore structure. This gated mechanoacid is incorporated via radical co-polymerization into linear and network polymers. Sonication experiments confirm the mechanical release of HCl, and single-molecule force spectroscopy reveals enhanced single-molecular toughness in the covalent strand. These mechanochemical functions are incorporated into a double-network hydrogel, leading to mechanically robust and thermally stable materials that undergo strain-triggered acid release. Both quasi-static stretching and high strain rate uniaxial compression result in substantial acidification of the hydrogel, from pH ~7 to ~5.

New concepts

This work demonstrates a new hierarchical approach to mechanoresponsive hydrogels. The structure of double-network polymeric hydrogels provides a mechanochemically active first network scaffold where mechanical stress is concentrated upon deformation. That stress is then transduced through a multi-stage chemical reaction cascade that both toughens the molecular strands of the first networks and generates HCl that is released into the hydrogel. Previous work on mechanochemically triggered changes in the bulk properties of double-network hydrogels has relied on strand scission events that are associated with compromised mechanical properties and that generate a single initial chemical product per chain. In contrast, the work reported here relies on strand extension events that are associated with improved mechanical properties and that generate multiple responses per chain. The combination of network and molecular design is shown to enable previously unattained levels of mechanochemical transduction for a synthetic system that recovers its initial shape after a strain-triggered event, suggesting new designs for mechanoresponsive materials.

Introduction

Recent years have seen the potential of covalent mechanochemical responses in polymers beginning to be realized in responsive material properties.[1–5] Examples of molecular responses include, but are not limited to, stress-induced color changes,[4,6–9] stress-strengthening,[10–12] triggered degradation,[13–15] and the release of chemical cargo.[16–21] Pervasive challenges in molecule-to-material translation include the need for material platforms that recover their desired shape even after experiencing the large strains that are necessary to trigger widespread mechanochemical transduction, especially for reactions that require large forces to achieve useful rates. The ways in which molecular events are transduced to a material outcome are highly varied, and they comprise a range of what might be characterized as either

Department of Chemistry, Duke University, Durham, North Carolina 27708, United States
E-mail: stephen.craig@duke.edu
†Electronic Supplementary Information (ESI) available. : [details of any supplementary information available should be included here]. See DOI: 10.1039/x0xx00000x
‡T. Ouchi and B. H. Bowser contributed equally to this work.

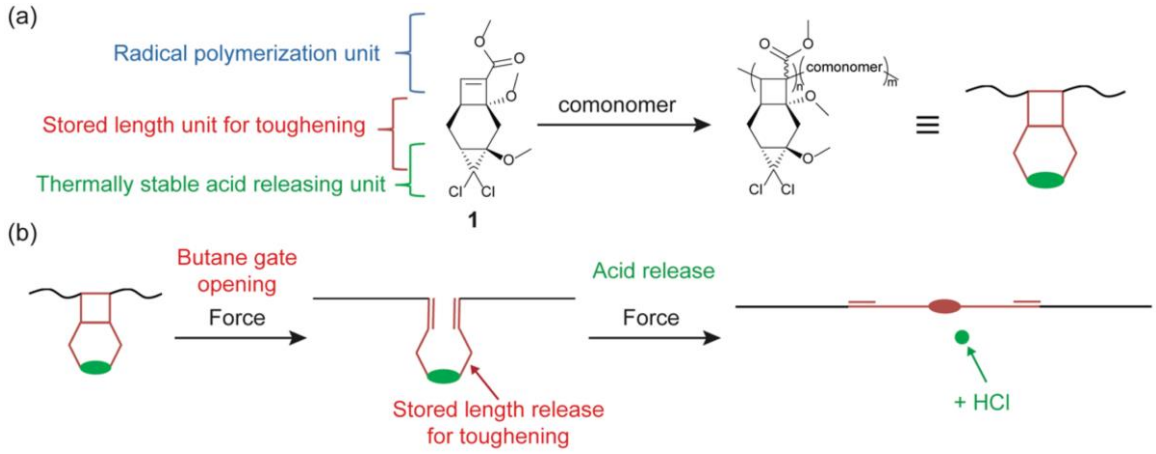

Fig. 1. (a) Design of the gated mechanoacid monomer and (b) its mechanochemical responses

direct or indirect pathways. By direct pathways, we refer to systems in which the mechanochemical reaction itself changes material properties. Representative examples include mechanochromic molecules, which change material color or luminescence through mechanochemical transformations,[2,4] and the controlled scission or extension of stress-bearing mechanophores that directly impact the tearing or stretching of the networks into which they are incorporated.[22–24] By indirect pathways, we refer to systems in which initial mechanochemical responses generate species that go on to react in a way that has macroscopic consequences. For example, the mechanochemical generation of protons,[25–27] radicals,[10] catalysts,[28] or reactive ene structures[12] can be coupled to polymerization/crosslinking reactions[10–12] or color changes brought about by subsequent acid-base reactions.[25] The release of new chemical species holds, in principle, the potential to transform the chemical environment throughout a mechanochemically coupled material and motivates the development of material systems that are mechanically robust and shape resistant, while also producing multi-functional chemical activity in response to an external load.

The proton is among the most broadly useful chemical species, motivating the elegant design and synthesis of mechanoacids based on *gem*-dichlorocyclopropane (*g*DCC)[29] and oxime sulfonate mechanophores by Moore and co-workers.[26,27] More recently, a mechanoacid derived from a 2-methoxy-substituted *gem*-dichlorocyclopropane (MeO-*g*DCC) was reported by Lin et al.; it combines ease of synthesis, thermal stability, and the ability to achieve detectable levels of activation in a shape-persistent elastomer.[25] These characteristics suggested that more dramatic responses, such as the rapid, strain-triggered acidification of hydrogels, might be possible if the aforementioned challenges of efficient, large-scale activation and shape recovery were addressed. Because hydrogels are typically fragile and therefore unlikely to accommodate strain-induced mechanochemical transduction before failing, we set out to incorporate the mechanoacid functionality into robust double-network hydrogels (DNs)[10,22,30] and to combine it with the toughening provided by reactive strand extension (RSE), which converts chain scission events into released stored length that recently has been reported to enhance DN toughness.[22] In addition, we hoped to combine RSE and acid release with other desirable attributes: (i) scalable synthesis of both mechanophore and polymer, (ii) thermal (force-free) stability, and (iii) a mechanically robust material platform that realizes efficient mechanophore activations, efficient dissociation of generated aid, and fast proton diffusion, while keeping its resilience in shape. Here, we report a mechanically robust, shape persistent hydrogel that meets these criteria and changes its pH in response to large, externally applied deformations.

Our design is shown in Fig. 1. Fused-ring monomer **1** incorporates four functions: radical polymerizability, substantial stored length for RSE toughening, mechanically triggered acid release, and thermal stability. The radical polymerizability is provided by the cyclobutene acrylate, and it enables the incorporation of multiple mechanoacids into a polymer chain with other comonomers.[22,31–35] The addition converts the cyclobutene into a cyclobutane mechanophore that functions as a mechanical gate to release the stored length of the fused cyclohexane upon mechanochemical activation. Further stretching enables the force activation of the thermally stable, gated MeO-*g*DCC unit, releasing HCl right after opening the gate. Here, we report the synthesis of the desired polymers, their characterization by both sonication and single-molecule force spectroscopy (SMFS), and their incorporation in DN hydrogels and subsequent activation in macroscopic materials.

Results and Discussion

Monomer synthesis

Monomer **1** was synthesized as described in Scheme. 1a. A 1,5-dimethoxy-1,4-cyclohexadiene core was chosen as the source of stored length, as we reasoned that the low ring strain of the six-membered ring might maintain the inherent thermal stability of the fused mechanoacid. The latter functionality is provided by a MeO-*g*DCC based on the work of Lin,[25] and it was introduced through dichlorocyclopropanation of one of the electron-rich alkenes. Subsequent cycloaddition of the other alkene with methyl propiolate installed a cyclobutene

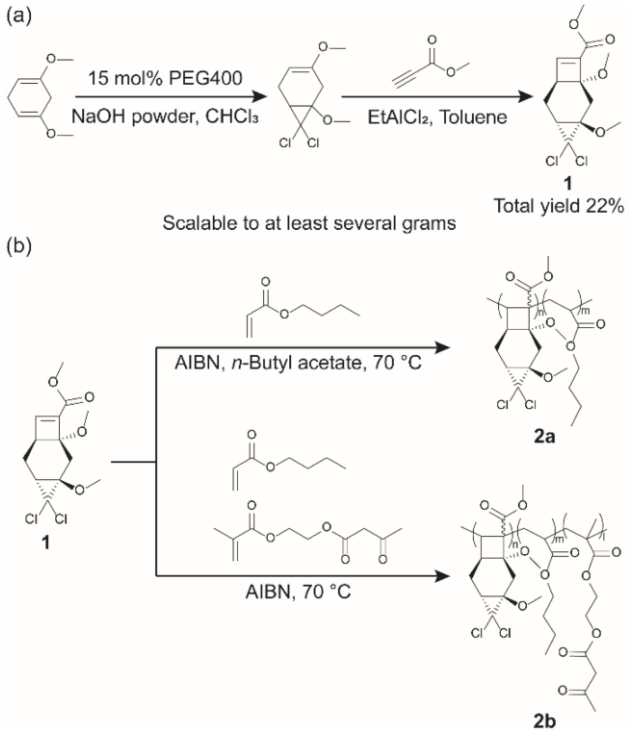

Scheme. 1. Synthesis of (a) gated mechanoacid monomer **1** and (b) polymers incorporating **1**. The stereochemistry of **1** is described in the ESI; the stereochemistries and tacticities of **2a** and **2b** that develop during polymerization are undetermined due to their complex NMR signals.

methacrylate unit for radical polymerization (see ESI for stereochemical assignments, Fig. S1-S5).[22,31–35] The synthesis of **1** requires only two steps, and it is easily scalable to at least several grams, which enables bulk material investigations.

Linear polymer synthesis

The gated mechanoacid was incorporated into a linear polymer chain through a conventional free radical polymerization (Scheme. 1b). Two copolymers were synthesized with azobisisobutyronitrile (AIBN) initiator at 70 °C - one each for subsequent mechanochemical reactivity analyses using sonication and single-molecule force spectroscopy (SMFS). Specifically, **1** was copolymerized with *n*-butyl acrylate (*n*BA) to provide copolymer (**2a**) for the sonication experiments, and copolymer **2b** was synthesized from **1**, *n*BA, and a 2-acetoacetoxyethyl methacrylate (AAEMA) co-monomer whose incorporation provided sufficiently strong attachments to an amine-functionalized AFM tip to enable SMFS.[22] For both polymers, **1** was successfully incorporated into polymer chains of high molecular weight: **2a**, M_n = 65 kDa, 9 mol% **1** (feed = 30 mol%); **2b**, 446 kDa, 4 mol% **1** (feed = 10 mol%) (See Table 1).

Mechanochemical activity

We tested the mechanochemical activity of **2a** and **2b** through sonication and single-molecule force spectroscopy (SMFS) studies, respectively. Sonication of **2a** (2 mg mL^{-1} solution in THF under 20 kHz; 1 s on and 1 s off) leads to the expected reduction in polymer molecular weight as the elongational forces generated during cavitation trigger chain scission (Fig. 2a). The extent of chain scission increases with sonication, as does the concurrent activation of the gated mechanophores. During the activation process, we expect that the butane gate first opens through a mechanochemical cycloreversion,[31] which transfers tension to the initially gated MeO-*g*DCC. The newly coupled tension in turn accelerates the ring-opening reaction of the MeO-*g*DCC and the subsequent elimination of HCl.[25] Based on previous reports,[25,31] we anticipated multiple products, including those shown in Fig. S16a, each of which has in turn up to 16 E/Z stereoisomers due to the formation of a total of 4 alkenes through the mechanochemical reactions. Additional structural complexities come into play as a result of polymer microstructure (e.g., head-tail configuration, various diad combinations). Consistent with these expectations, the ^{1}H NMR spectrum of the sonicated polymer is (perhaps euphemistically) complex. These features make it difficult to conclusively assign each proton peak. However, the spectrum bears new peaks at δ = 6.4 ppm and 6.3 ppm that increase with sonication time and are consistent with the desired formation of vinyl protons (Fig. S11). Furthermore, the UV-vis absorption spectrum shows a red-shifted peak at λ_{max} = 296 nm that similarly increases with sonication time and is characteristic of the formation of conjugated π systems (Fig. S12).

The precise structure of sonicated **2a**, however, is secondary to the desired generation of HCl, which was confirmed through the use of the acid indicator rhodamine B. When added to the unsonicated **2a** solution, rhodamine B remains colorless (Fig. 2b). Addition to the sonicated solutions (which are otherwise colorless), however, leads to a rich pink color that is typical of the protonation of rhodamine B. The production of acid is verified by UV-vis absorption spectroscopy; the spectrum of the sonicated polymer + indicator solution matches that of protonated rhodamine B, and the intensity of the absorbance increases with sonication time (Fig. S13).

Table 1. Summary of the polymers used for sonication (**2a**) and SMFS (**2b**) experiments

	Incorporation ratio[a)]			*M*n (g mol^{-1})[b)]	*M*w (g mol^{-1})[b)]	*M*z (g mol^{-1})[b)]	*Đ*
	Gated mechanoacid	*n*BA	AAEMA				
2a	0.09	0.91	-	64,700	179,000	360,000	2.76
2b	0.04	0.78	0.19	446,000	2,150,000	11,400,000	4.81

[a)] ^{1}H NMR; [b)] GPC-MALS

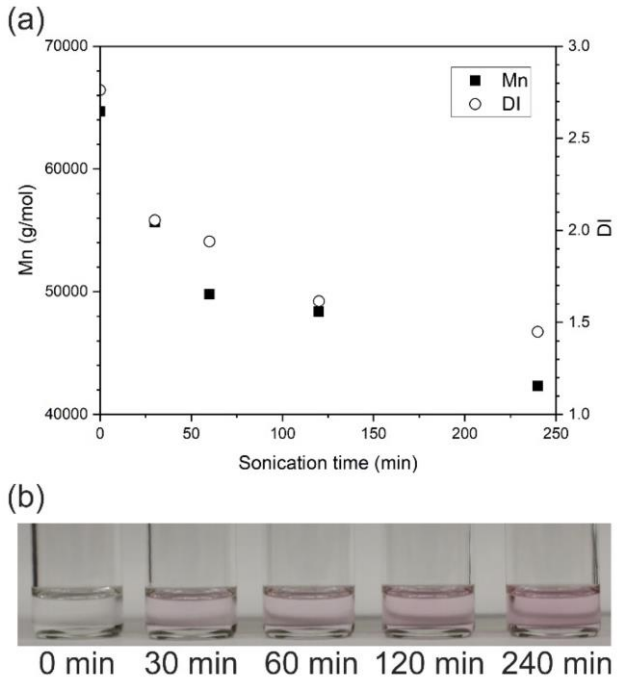

Fig. 2. HCl generation by sonication: (a) molecular weight and dispersity index changes during sonication, and (b) color change of rhodamine B solutions. 0.9 mL of the sonicated solutions were injected into 0.1 mL of 2 mM rhodamine B in THF.

The mechanochemical activity and the RSE behavior of the polymer were further characterized by SMFS of **2b**, using procedures established previously in our lab.[22,36–39] The AAEMA co-monomer enables high-force adhesion between the polymer and an amine-functionalized AFM tip, presumably through the formation of a vinylogous urea linkage. As seen in the SMFS curves shown in Fig. 3, the polymer exhibits the following behaviors that are typical of a flexible polymer chain up to forces of ~2,000 pN: (i) initial linear response that is associated with low force extension (~1 to 10s of pN) due to entropic distortion; (ii) a transition as the polymer end-to-end distance reaches its fully extended contour length (order of 10^2 pN); (iii) a second, steeper linear response (several hundred pN and higher) that is dominated by enthalpic distortion along the polymer backbone (e.g., bond bending and bond stretching). Without the fused cyclohexyl ring to provide stored length (i.e., a monocyclic cyclobutane), the polymer chain would break and cease to be stress-bearing at forces of approximately 2,000 pN, where the cyclobutane breaks under these loading conditions.[22] Instead, the fused rings in the gated mechanoacid enable the release of stored length that results in a characteristic plateau in the SMFS force-extension curve (Fig. 3). This covalent chemical structural transition converts a two-bond repeat along the polymer backbone into a total of nine bonds. The resulting extension (RSE) occurs at high force (2,000-2,500 pN) and provides additional molecular toughness at the single-molecule level; a similar response has been shown to translate to the macroscopic properties of double-network hydrogels.[22] The measured transition force is typical of, but slightly higher than, reported cyclobutane ring openings, and it is much greater than that observed previously for MeO-*g*DCC mechanoacid (880

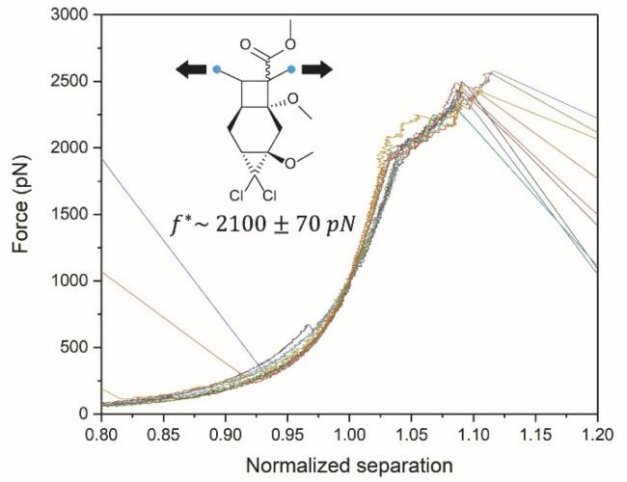

Fig. 3. Representative normalized SMFS curves. $f^*$is the activation force near the center of the plateau in the force-separation curve, and the separation is normalized relative to separation at force = 1,000 pN.

pN).[25] We therefore expect that the activation of each acid generating MeO-*g*DCC immediately follows the activation of its cyclobutane ring opening, as reported for a similar system previously.[40] The fused MeO-*g*DCC has a very small, if any, effect on cyclobutane reactivity in comparison to substituents directly on the cyclobutane ring.[39]

Incorporation into double-network (DN) hydrogels

With its activity established, we incorporated the mechanophore into DN hydrogels in pursuit of large scale, strain triggered activation and acidification with full shape recovery. DN gels comprise a fully-swollen, overstretched 1st network and a loosely crosslinked 2nd network. DNs are known for their exceptionally high toughness under mechanical loading, where the 1st network serves as a stress-bearing component that fragments at lower strains through bond scission events, whereas the interpenetrating 2nd network holds the DN together and provides resilience.[41] Recently, the targeted loading of the first network has been exploited for efficient activation of mechanophores incorporated into the first network.[10,22,30,41–43] Here, **1** (feeding ratio of 20 mol%) was copolymerized with 2-acrylamido-2-methyl-1-propanesulfonic acid sodium salt (NaAMPS) and *N*,*N*'-methylenebis(acrylamide) (BisAAm) crosslinker to form a single network (SN) in dimethyl sulfoxide (DMSO) through conventional free radical polymerization (Fig. 4a). 20 mol% of monomer **1** is the highest feed ratio with which we were able to realize a well-formed 1st network. Higher **1** content led to solubility issues in DMSO and less well-formed networks, presumably due to its steric hindrance and/or the hydrogen abstraction from the carbon alpha to the acrylate during the radical polymerization, as seen in previous studies.[22,31].[22,31] After exchanging the solvent to water, the SN was immersed into a solution of acrylamide (AAm), BisAAm crosslinker, and initiator (Fig. 4b). Subsequent free radical polymerization led to the in-situ formation of a second, loosely crosslinked acrylamide network that interpenetrates the mechanochemically active first network. The resulting DN hydrogel was immersed in an aqueous solution

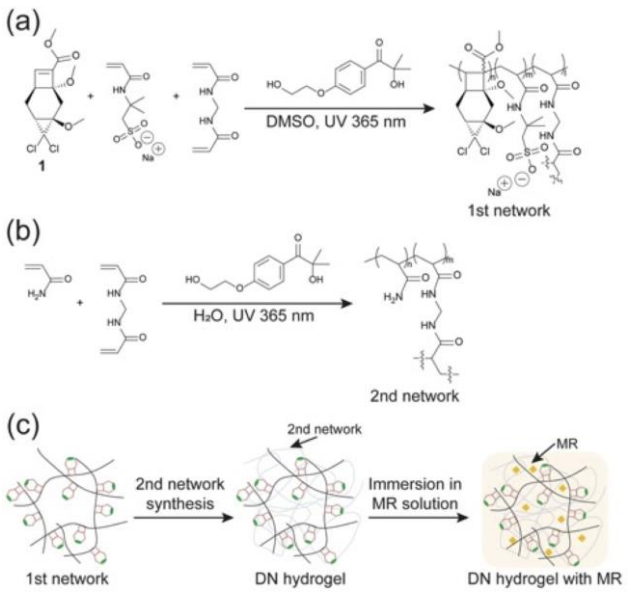

Fig. 4. DN hydrogel preparation: (a) chemical structures of the 1st network, (b) chemical structures of the 2nd network, and (c) simplified preparation scheme of the DN hydrogel.

of 0.3 mM methyl red (MR), which functioned as a pH indicator to signal the generation of acid (Fig. 4c).

The force-free thermal stability of the gated mechanoacid within the hydrogel was confirmed by immersing the DN in a 0.3 mM MR aqueous solution. No measurable change in pH is observed over 4 weeks at room temperature, and at elevated temperature the mechanophore showed greater stability than that intrinsic to the double network itself (see ESI for details, Fig. S24 and S25 and Table S10 and S11). Room temperature stability is an important characteristic for practical applications, and we were gratified to observe that the introduction of stored length via the doubly-fused hexane ring does not compromise the force-free stability of the acid releasing unit.

Activation under high strain rate uniaxial compression

A biaxial stretching with a high strain rate was applied to the DN hydrogel by hammer strikes (Fig. 5). This DN hydrogel shows tough material's responses. It recovers its original shape after hammer strikes and no apparent fracture is observed. Furthermore, the color of the DN immediately changes from yellow to pink right after a hammer strike (Fig. 5a and Video S1, real time), indicating HCl release under mechanical stimuli and subsequent protonation of methyl red (MR) pH indicators (Fig. 5c). The instantaneous color change (less than a second) is much faster than observed previously for ungated MeO-*g*DCC in PDMS,[25] where limiting diffusion in the elastomer leads to gradual color change from a RhB indicator over the course of minutes or hours. Even with the staged activation of the mechanophore and the subsequent bimolecular, indirect pathway for protonation at play here, the response rate of this DN hydrogel system is closer to that seen in direct mechanochromic pathways, such as spiropyran (SP) mechanophore systems (e.g., SP in PDMS) in which an instantaneous color change (less than a second) results from

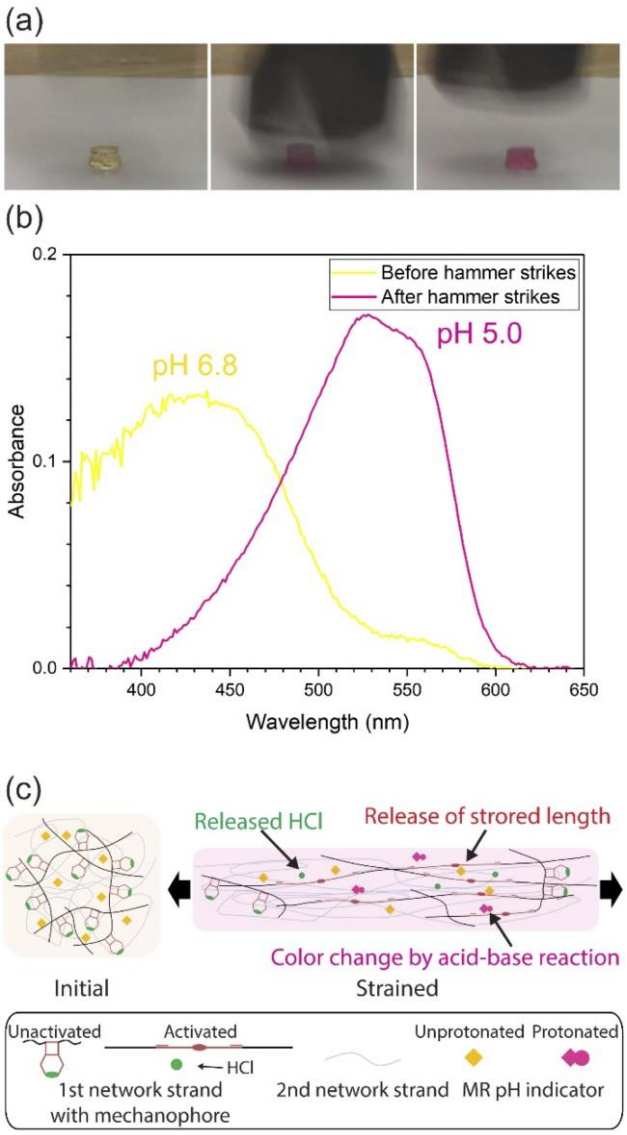

Fig. 5. DN hydrogel under high strain rate uniaxial compression: (a) consecutive video frames of a DN hydrogel during a hammer strike (interval of 0.033 s, or 30 frames per second), (b) UV-vis spectra (sample ID DN-1 in Table S8), and (c) schematic picture of DN molecular structures before and during mechanical loading. Both UV-vis spectra were processed to minimize the effects of scattering: the spectrum before hammer strikes is corrected by subtracting the constant absorbance value at 635 nm from the spectrum, while that of after hammer strikes is the corrected absorbance spectrum with fitting function taking into account scattering effects. The pH is calculated based on a calibration curve (see details for both UV-vis and pH analyses in the ESI, Fig. S18-S22, and Table S7 and S8).

the mechanochemically coupled unimolecular conversion of SP to merocyanine (MC).[6,9] The rapid kinetics in the present system are presumably due to the much faster diffusion of protons in the aqueous environment of the DN hydrogel relative to silicone elastomers, highlighting one aspect of the potential of mechanoacids as transducers of macroscopic mechanical signals.

The acidification of the DN hydrogel was quantified by UV-vis spectroscopy. The equilibrium ratio of protonated to unprotonated methyl red (MR) was characterized by the relative absorbance at 530 nm vs. 440 nm, where the longer

wavelength is dominated by the protonated form of the indicator. A calibration curve of A_{530}:A_{440} as a function of pH was determined through titration of HCl into a pre-gel solution (see ESI for details, Fig. S18 and S19). A cylinder (diameter = 8 or 12 mm and thickness = ~2.5 mm) was made with a biopsy punch. The nascent, yellow sample exhibits a large peak at 440 nm, consistent with predominately unprotonated MR, and an associated pH of 6.76 ± 0.01. The sample was then struck multiple (~60) times with a hammer to evenly distribute activation and color throughout the cylinder. After hammer strikes, a distinct color change from yellow to pink is observed (Fig. 5a), and the absorbance at 530 nm becomes dominant (Fig. 5b). Comparison with the calibration curve gives a final pH of 4.96. A similar drop in pH is observed when the as-made DN is immersed in a basic solution of sodium hydroxide to raise the initial pH to 7.3–7.4. After repeated hammer strikes, the pH drops to 5.2–5.4, or a roughly hundred-fold increase in proton concentration (see Fig. S22 and Table S8). On the other hand, the control DN hydrogel, which contains a mechanically uncoupled small molecule analog of the mechanoacid, shows no significant change in its UV-vis spectrum and corresponding pH in response to repeated hammer strikes (see the details on the control experiments in ESI, Fig. S23). These results further support that the acidification is induced through the mechanochemical reactions. The observed pH drop from ~7 to ~5 is comparable to that exploited in biology through endocytosis, where extracellular substances are taken inside a cell through the formation of a vesicle; a pH of 6–7 in the early stage of endocytosis drops to 5 at the late stage of the endocytic compartment.[44–46] This range of pH drops is used in cells to regulated ligand-receptor (un)binding, pointing to future opportunities to couple the mechanochemical response observed here to biologically inspired systems of feedback and regulation.

The titrations used to generate the spectroscopic calibration curves also provide a basis for determining the extent of mechanophore activation, taking into account buffering effects due to the polymer network. The amount of released HCl required to generate the observed pH drop from 6.8 to 5.0 was calculated by comparison to the titration data determined through titration and found to be 1.70 ± 0.01% of the total mechanophore loading of the DN (including any unreacted mechanically inactive mechanophore). This level of activation is almost an order of magnitude greater than reported previously for activation in a silicone elastomer (0.18%),[25] despite a much higher activation force (i.e., SMFS thresholds of 880 pN in the previous case vs. 2,100 pN here). Generally, inefficient mechanophore activation inside a bulk material has been a bottleneck to mechanophore-based responsive material development.[4] This is mainly due to an inhomogeneous molecular force distribution originating from the heterogeneities intrinsic to non-crystalline polymer networks.[47,48] Even lower fractional activation of dioxetane mechanophores (0.03%) were reported by Clough et al. in a similar silicone elastomer,[49] and activation of 1.7% is quite high by comparison. Fractional activations above 1.70 % have been reported only in melts with large plastic deformation[50] or multiple-network systems.[16,43,51]

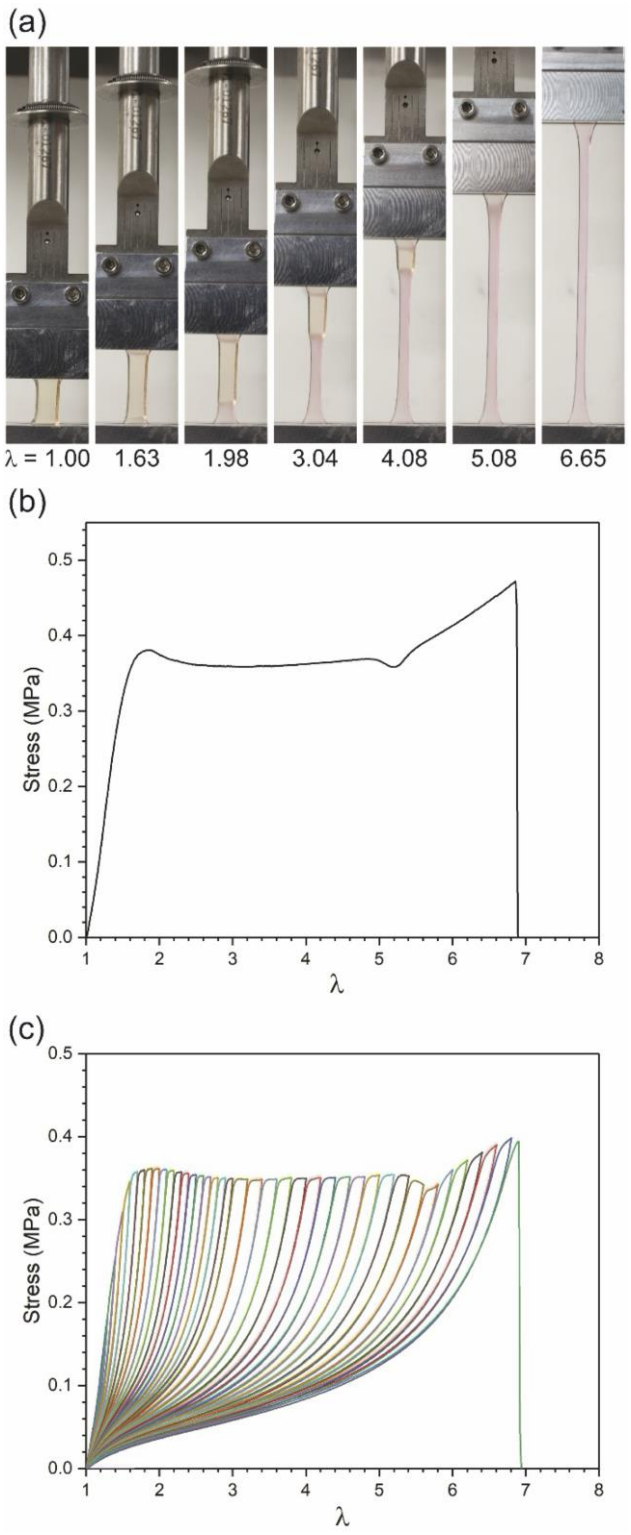

Fig. 6. Mechanical testing of a DN hydrogel incorporating gated mechanoacid: (a) DN hydrogel at different uniaxial stretch: pink color indicates the protonation of methyl red pH indicator due to the activations of gated mechanoacids; (b) tensile test; (c) cyclic loading test.

Activation under quasi-static tension

The mechanochemical response of the DN hydrogel was characterized under the more controlled and quantitative loading of quasi-static, uniaxial tension. In the resulting stress-strain curves, a clear yielding at 0.38 MPa is observed at an extension ratio (λ) of approximately 1.85 (i.e., 85 % strain), corresponding to necking of the sample (Fig. 6b). This yielding behavior is a signature of a tough DN; it indicates well-formed networks and an effective stress redistribution from the first network to the second network while the first is strained to the point of fracture as shown in the large hysteresis due to its energy dissipation under cyclic loadings (Fig. 6c). The ability to achieve high regions of (over)stressed strands throughout the DN enables widespread mechanophore activation.[22,41] Indeed the necked regions of the DNs show a distinct color change from pale yellow to pink (Fig. 6a), demonstrating that the mechanochemical reactions are efficiently induced in this necked region, where high molecular tensions are well-distributed. Further stretching causes both the neck and the pink color to propagate along the sample, while the stress remains almost constant. Once the necked area propagates across the entire sample, a dip in stress is observed around λ = 5.2, as seen in previous DN hydrogel systems.[10,41] Then, strain hardening starts to occur, and the entire sample turns pink (see detailed RGB image analysis in Fig. S17, Video S2). The pH undergoes a cumulative drop from 6.36 ± 0.01 to 5.59 ± 0.17, corresponding to mechanophore activation of 0.83 ± 0.12%, after break. As with the uniaxial compression delivered by the hammer strikes, quasi-static tensile loading results in efficient mechanophore and a significant drop in pH. It should be also noted that the DN hydrogel shows a highly elastic response due to its second network regardless of this hysteresis: each cycle showed only minimal permanent strain (less than 2% strain in the cyclic test).

Conclusions

The mechanoacid monomer **1** combines four functions: 1) radical polymerizability, 2) covalently stored length for toughening, 3) thermal stability, and 4) mechanically triggered acid release. Firstly, this radical polymerizability enables the incorporation of this gated mechanoacid into polymer backbone with desired functional comonomers. This means that a high incorporation would be possible without deviations from both a target elastic modulus and an aimed material toughness, while previous mechanoacid molecules were incorporated mainly as crosslinkers that inherently alter elastic modulus and sacrifice material toughness with the increase in their incorporation ratios.[25,26] Secondly, the covalently stored length increases molecular toughness through reactive strand extension (RSE) mechanism. This gated mechanoacid has a high activation force of ~2,100 pN with the large extension ratio (length after RSE/before RSE) per molecule, which is comparable to the previous work where two-fold in material toughness was realized through RSE.[22] Due to synthetic complexities, we were unable to generate an appropriate control DN in this case to directly quantify the toughening effects of RSE in this specific bulk material, but the similarity in molecular and DN designs suggest that similar toughening effects should be induced in the present DN hydrogel as have been reported in a previous study.[22] Thirdly, the thermal stability of the gated mechanoacid is beneficial for practical applications. The combination of radical polymerizability and thermal stability enables the fabrication of a mechanically robust DN hydrogel. The ionic comonomer allows for an efficient pre-stretching of the 1st network with the mechanoacids through a high osmotic pressure, enabling almost one order higher mechanophore activations despite the high activation force of this mechanoacid (~2,100 pN). To the best of our knowledge, this is the first example of activated mechanophores that require such high activation forces in shape-recoverable bulk materials.

Looking ahead, the mechanically triggered acid release might enable a variety of opportunities through indirect pathways. Whereas direct pathways produce immediate responses and offer direct correlations between molecular and material behavior, indirect pathways offer the possibilities of (i) coupling a given mechanophore activation to a range of potential material changes, by choosing a secondary reaction to meet a target property, and (ii) amplification of the mechanophore response, for example through the generation of a catalyst or initiator of subsequent reactivity. In the DN hydrogels, the speed of the acid-base reaction is comparable to that observed through mechanochemical reactions with a direct pathway, such as the color change associated with spiropyran activation in a PDMS elastomer.[6,9] Not only the speed, but the magnitude, of the response is notable. The observed pH drop from ~7 to ~5, or roughly a 100-fold increase in proton concentration, is similar to that observed in biology during endocytosis.[44–46] The proton is one of the most versatile and useful chemical species: it stoichiometrically reacts with other species (e.g., acid-base reactions), catalytically triggers a wide range of reactions, and pH changes have a huge impact on various kinds of biological/physical phenomena, such as enzymatic activities,[52] phase transitions,[53] and swelling of gels.[54] The radical polymerizability of the gated mechanoacid enables its facile incorporation with acid-responsive functional groups through copolymerization. For example, acid-catalyzed polymerization/crosslinking reactions might induce stress-strengthening and/or toughening that compete with destructive bond scission events; acid-catalyzed depolymerization could lead to strain-triggered degradable networks; and enzymatic activities inside a gel might be switched on or off in response to pH changes. Variations on the platform reported here offer an opportunity to explore such possibilities.

Finally, adding reversibility or reusability in the mechanochemical reactions represents an interesting future direction. The chemistry used in this study is not reversible once the strain is released. Similar opened cyclobutane gates, however, could be reformed through cyclization reaction.[55] Also, the diene generated by the mechanochemical reaction could be a useful reactant for the addition of further stored length and/or acid releasing units.[25,31,56]

Author Contributions

T.O., B.H.B. and S.L.C. conceived the project. T.O., B.H.B., and S.L.C designed the experiments. T.O. and B.H.B. performed the syntheses and structural characterization of the small molecules and the linear polymers. T.O. and B.H.B. conducted the experiments and analysis of the sonication study. T.B.K. conducted the SMFS experiments, and T.O. and B.H.B. performed the analysis of the SMFS and associated calculations. T.O. synthesized the DN hydrogels and performed the experiments on and analysis of the DN hydrogels. T.O., B.H.B., T.B.K., X.Z., and S.L.C. discussed the results. S.L.C. provided the funding. T.O., B.H.B., and S.L.C. wrote the manuscript.

‡T. Ouchi and B. H. Bowser contributed equally to this work.

Conflicts of interest

The authors declare no conflict of interest.

Acknowledgements

This work is supported by the US Army Research Office (Grant No. W911NF-20-2-0182) and Duke University. The authors thank Dr. Benjamin Bobay for assistance with the NMR analyses and Dr. Peter Silinski for assistance with the mass spectrometry analyses.

Notes and references

1 M. A. Ghanem, A. Basu, R. Behrou, N. Boechler, A. J. Boydston, S. L. Craig, Y. Lin, B. E. Lynde, A. Nelson, H. Shen and D. W. Storti, *Nat. Rev. Mater.*, 2021, **6**, 84–98.

2 J. Li, C. Nagamani and J. S. Moore, *Acc. Chem. Res.*, 2015, **48**, 2181–2190.

3 B. H. Bowser and S. L. Craig, *Polym. Chem.*, 2018, **9**, 3583–3593.

4 N. Deneke, M. L. Rencheck and C. S. Davis, *Soft Matter*, 2020, **16**, 6230–6252.

5 J. Ribas-Arino and D. Marx, *Chem. Rev.*, 2012, **112**, 5412–5487.

6 Y. Lin, M. H. Barbee, C. C. Chang and S. L. Craig, *J. Am. Chem. Soc.*, 2018, **140**, 15969–15975.

7 D. A. Davis, A. Hamilton, J. Yang, L. D. Cremar, D. Van Gough, S. L. Potisek, M. T. Ong, P. V. Braun, T. J. Martínez, S. R. White, J. S. Moore and N. R. Sottos, *Nature*, 2009, **459**, 68–72.

8 Y. Chen, A. J. H. Spiering, S. Karthikeyan, G. W. M. Peters, E. W. Meijer and R. P. Sijbesma, *Nat. Chem.*, 2012, **4**, 559–562.

9 G. R. Gossweiler, G. B. Hewage, G. Soriano, Q. Wang, G. W. Welshofer, X. Zhao and S. L. Craig, *ACS Macro Lett.*, 2014, **3**, 216–219.

10 T. Matsuda, R. Kawakami, R. Namba, T. Nakajima and J. P. Gong, *Science*, 2019, **363**, 504–508.

11 A. L. B. Ramirez, Z. S. Kean, J. A. Orlicki, M. Champhekar, S. M. Elsakr, W. E. Krause and S. L. Craig, *Nat. Chem.*, 2013, **5**, 757–761.

12 J. Wang, I. Piskun and S. L. Craig, *ACS Macro Lett.*, 2015, **4**, 834–837.

13 Y. Lin, T. B. Kouznetsova and S. L. Craig, *J. Am. Chem. Soc.*, 2020, **142**, 2105–2109.

14 Y. Lin, T. B. Kouznetsova, C. C. Chang and S. L. Craig, *Nat. Commun.*, 2020, **11**, 1–9.

15 T. G. Hsu, J. Zhou, H. W. Su, B. R. Schrage, C. J. Ziegler and J. Wang, *J. Am. Chem. Soc.*, 2020, **142**, 2100–2104.

16 P. B. Jayathilaka, T. G. Molley, Y. Huang, M. S. Islam, M. R. Buche, M. N. Silberstein, J. J. Kruzic and K. A. Kilian, *Chem. Commun.*, 2021, **57**, 8484–8487.

17 M. B. Larsen and A. J. Boydston, *J. Am. Chem. Soc.*, 2013, **135**, 8189–8192.

18 M. B. Larsen and A. J. Boydston, *J. Am. Chem. Soc.*, 2014, **136**, 1276–1279.

19 X. Hu, T. Zeng, C. C. Husic and M. J. Robb, *J. Am. Chem. Soc.*, 2019, **141**, 15018–15023.

20 Y. Sun, W. J. Neary, Z. P. Burke, H. Qian, L. Zhu and J. S. Moore, *J. Am. Chem. Soc.*, 2022, **144**, 1125–1129.

21 H. Shen, M. B. Larsen, A. G. Roessler, P. M. Zimmerman and A. J. Boydston, *Angew. Chemie - Int. Ed.*, 2021, **60**, 13559–13563.

22 Z. Wang, X. Zheng, T. Ouchi, T. B. Kouznetsova, H. K. Beech, S. Av-Ron, T. Matsuda, B. H. Bowser, S. Wang, J. A. Johnson, J. A. Kalow, B. D. Olsen, J. P. Gong, M. Rubinstein and S. L. Craig, *Science*, 2021, **374**, 193.

23 S. Wang, H. K. Beech, B. H. Bowser, T. B. Kouznetsova, B. D. Olsen, M. Rubinstein and S. L. Craig, *J. Am. Chem. Soc.*, 2021, **143**, 3714–3718.

24 S. J. Bailey, C. W. Barney, N. J. Sinha, S. V. Pangali, C. J. Hawker, M. E. Helgeson, M. T. Valentine and J. Read de Alaniz, *Mater. Horizons*, 2022, 1947–1953.

25 Y. Lin, T. B. Kouznetsova and S. L. Craig, *J. Am. Chem. Soc.*, 2020, **142**, 99–103.

26 C. E. Diesendruck, B. D. Steinberg, N. Sugai, M. N. Silberstein, N. R. Sottos, S. R. White, P. V. Braun and J. S. Moore, *J. Am. Chem. Soc.*, 2012, **134**, 12446–12449.

27 C. Nagamani, H. Liu and J. S. Moore, *J. Am. Chem. Soc.*, 2016, **138**, 2540–2543.

28 A. Piermattei, S. Karthikeyan and R. P. Sijbesma, *Nat. Chem.*, 2009, **1**, 133–137.

29 J. M. Lenhardt, A. L. Black and S. L. Craig, *J. Am. Chem. Soc.*, 2009, **131**, 10818–10819.

30 Z. J. Wang, J. Jiang, Q. Mu, S. Maeda, T. Nakajima and J. P. Gong, *J. Am. Chem. Soc.*, 2022, **144**, 3154–3161.

31 B. H. Bowser, C. H. Ho and S. L. Craig, *Macromolecules*, 2019, **52**, 9032–9038.

32 J. H. K. Hall and P. Ykman, *J Polym Sci Macromol Rev*, 1976, **11**, 1–45.

33 T. Kitayama, T. Kawauchi, N. Ueda, C. S. Kniep, W. S. Shin, A. B. Padias and J. H. K. Hall, *J. Macromol. Sci. Part A - Chem.*, 1967, **1**, 569–579.

34 E. Ihara, T. Ueda, K. Yokoyama, Y. Fujiwara, K. Inoue, T. Itoh, H. Shimomoto, H. Momose and M. Nodono, *J. Polym. Sci. Part A Polym. Chem.*, 2013, **51**, 2716–2724.

35 X. Chen, B. A. Sufi, A. B. Padias and J. H. K. Hall, *Macromolecules*, 2002, **35**, 4277–4281.
36 T. B. Kouznetsova, J. Wang and S. L. Craig, *ChemPhysChem*, 2017, **18**, 1486–1489.
37 H. M. Klukovich, T. B. Kouznetsova, Z. S. Kean, J. M. Lenhardt and S. L. Craig, *Nat. Chem.*, 2013, **5**, 110–114.
38 J. Wang, T. B. Kouznetsova, Z. Niu, M. T. Ong, H. M. Klukovich, A. L. Rheingold, T. J. Martinez and S. L. Craig, *Nat. Chem.*, 2015, **7**, 323–327.
39 B. H. Bowser, S. Wang, T. B. Kouznetsova, H. K. Beech, B. D. Olsen, M. Rubinstein and S. L. Craig, *J. Am. Chem. Soc.*, 2021, **143**, 5269–5276.
40 J. Wang, T. B. Kouznetsova, R. Boulatov and S. L. Craig, *Nat. Commun.*, 2016, **7**, 1–8.
41 J. P. Gong, *Soft Matter*, 2010, **6**, 2583–2590.
42 J. P. Gong, Y. Katsuyama, T. Kurokawa and Y. Osada, *Adv. Mater.*, 2003, **15**, 1155–1158.
43 E. Ducrot, Y. Chen, M. Bulters, R. P. Sijbesma and C. Creton, *Science*, 2014, **344**, 186–189.
44 J. Gruenberg and F. R. Maxfield, *Curr. Opin. Cell Biol.*, 1995, **7**, 552–563.
45 S. Mukherjee, R. N. Ghosh and F. R. Maxfield, *Physiol Rev*, 1997, **77**, 759–803.
46 L. Ma, Q. Ouyang, G. C. Werthmann, H. M. Thompson and E. M. Morrow, *Front. Cell Dev. Biol.*, 2017, **5**, 1–18.
47 R. Adhikari and D. E. Makarov, *J. Phys. Chem. B*, 2017, **121**, 2359–2365.
48 M. Zhong, R. Wang, K. Kawamoto, B. D. Olsen and J. A. Johnson, *Science*, 2016, **353**, 1264–1268.
49 J. M. Clough, C. Creton, S. L. Craig and R. P. Sijbesma, *Adv. Funct. Mater.*, 2016, **26**, 9063–9074.
50 J. M. Lenhardt, A. L. Black, B. A. Beiermann, B. D. Steinberg, F. Rahman, T. Samborski, J. Elsakr, J. S. Moore, N. R. Sottos and S. L. Craig, *J. Mater. Chem.*, 2011, **21**, 8454–8459.
51 W. Qiu, P. A. Gurr and G. G. Qiao, *Macromolecules*, 2020, **53**, 4090–4098.
52 P. Li, Y. Zhong, X. Wang and J. Hao, *ACS Cent. Sci.*, 2020, **6**, 1507–1522.
53 G. Kocak, C. Tuncer and V. Bütün, *Polym. Chem.*, 2017, **8**, 144–176.
54 M. C. Koetting, J. T. Peters, S. D. Steichen and N. A. Peppas, *Mater. Sci. Eng. R Reports*, 2015, **93**, 1–49.
55 S. Poplata, A. Tröster, Y. Q. Zou and T. Bach, *Chem. Rev.*, 2016, **116**, 9748–9815.
56 B. B. Snider, D. J. Rodini, R. S. E. Conn and S. Sealfon, *J. Am. Chem. Soc.*, 1979, **101**, 5283–5293.